

Microbial Pb(II)-precipitation: the influence of oxygen on Pb(II)-removal from aqueous environment and the resulting precipitate identity

ArticleCategory : Original Paper

Copyright-Holder: Islamic Azad University (IAU)

Copyright-Year: 2019

H. G. Brink ^{1*}, C. Hörstmann ¹, J. Peens ¹

¹Department of Chemical Engineering, Faculty of Engineering, Built Environment and Information Technology, University of Pretoria, Private Bag X20, Hatfield, Pretoria, 0028, South Africa

Rec: 11 February 2019, Rev: 26 June 2019, Accp: 3 August 2019,

Abstract

The study aimed to quantify the lead(II) bio-precipitation effectiveness, and the produced precipitate identities, of industrial consortia under aerobic and anaerobic batch conditions. The consortia were obtained from an automotive battery recycling plant and an operational lead mine in South Africa. The experiments were performed in the complex growth medium Luria–Bertani broth containing 80 ppm lead(II). The precipitation and corresponding removal of lead(II) were successfully achieved for both aerobic (yellow/brown precipitate) and anaerobic (dark grey/black precipitate) conditions. The removal of lead(II) followed similar trends for both aeration conditions, with the majority of lead(II) removed within the initial 48 h, followed by a marked decline in removal rate for the remainder of the experiments. The final lead(II) removal ranged between $78.11 \pm 4.02\%$ and $88.76 \pm 3.98\%$ recorded after 144 h. The precipitates were analysed using XPS which indicated the presence of exclusively PbO and elemental lead in the aerobic precipitates, while PbO, PbS, and elemental lead were present in the anaerobic precipitates. The results indicated an oxidation–reduction mechanism with lead(II) as an electron acceptor in both aerobic and anaerobic conditions, while a sulphide-liberation catabolism of sulphur-containing amino acids was evident exclusively in the anaerobic runs. This study provides the first report of bacterial bio-reduction in aqueous lead(II) to elemental lead through a dissimilatory lead reduction mechanism. It further provides support for the application of bioremediation for the removal and recovery of lead from industrial waste streams through the application of bacterial biocatalysts for direct elemental lead recovery.

Keywords: Aerobic bioremediation, Anaerobic bioremediation, Dissimilatory lead reduction, Microbial bioremediation

Introduction

Various technologies depend on the availability of lead (Pb) for industrial applications, including storage battery plates, sheathing for electrical cables, small calibre ammunition, shielding for X-ray apparatus and atomic reactors, type metal, bearing metal, and solder. However, as opposed to many other metallic species, natural Pb-occurrence is not common on the earth's surface. In the earth's crust, Pb exists mostly as the sulphur compound galena (PbS). It is estimated that the world production of refined Pb from natural reserves is 5 million tons per year (International Lead Association [2018](#)). Workable raw Pb-reserves are estimated at 87 million tons—about 17 years' supply at the current rate of usage (Statista [2018](#)).

The high incidence of observed environmental Pb can mostly be attributed to human activity. Anthropogenic Pb is introduced through metal works and the use of products containing Pb-additives such as paints and

gasoline (Gioia et al. 2006). In car engines, the burning of fuel in the presence of other impurities (such as chlorines, bromines, and oxides) produces Pb-salts (Russell and Vincent 1998). Finally, Pb is released from the combustion of coal during electric power generation in coal-powered plants (Block and Dams 1975).

The Pb-recirculation caused by human sources is far more extensive than the natural Pb-cycle, causing Pb-pollution to be a worldwide problem (Bollhöfer and Rosman 2000; United Nations Environment Programme 2010). The increased non-localized localised outputs of Pb to the environment have generated a great deal of concern, mainly due to its toxicity to living organisms. Pb-contamination of water and land is known to produce sub-chronic effects at low concentrations (Supanopas et al. 2005), acute effects at moderately high concentrations (Papp et al. 2006), and catastrophic changes to ecosystems at very high concentrations (Eisler 1988). For example, Pb-concentrations under 10 mg/L can disrupt endocrine activity in sensitive species, while concentrations above 1000 ppm can eradicate entire ecosystems. Additionally, Pb tends to disproportionately impact vulnerable groups including children (Mathee et al. 2013; Oulhote et al. 2013; Taylor et al. 2013) and marginalised peoples (Barbosa et al. 2009). In the South African context, Pb-pollution predominantly affects economically disadvantaged communities. This typically results from Pb-containing paint peeling from unmaintained buildings and contaminating food and water supplies, the use of Pb-containing batteries as sinkers by subsistence fishermen, and the unregulated use of Pb in traditional medicines (Mathee et al. 2013; Mathee 2014; Mathee et al. 2015).

Conventional treatment technologies such as sand filtration, GAC adsorption, precipitation sedimentation, flotation, ion-exchange, and electrochemical deposition systems have been applied historically for the removal of the toxic heavy metals such as Cd, Pb, Fe, Mn, Cr, and As from water (Wang et al. 2004; Aziz et al. 2008). However, disadvantages of these processes include lack of selectivity, low efficiency, cost-intensive steps, and waste production, indicating the need for economically viable and environmentally conscious alternatives (Barbaro and Liguori 2009; Ngwenya and Chirwa 2010; Barakat 2011).

Several researchers have investigated the feasibility of biological processes to remove Pb from water and wastewater. Most of these studies have employed microorganisms as biosorbents using dead or reconditioned biomass (Adeniji 2004; Chatterjee et al. 2012; Singh et al. 2014; Manzoor et al. 2019). However, the use of living microorganisms promises significant advantages. For example, continuous catalyst production and active metabolic mechanisms may prove useful in bioremediation. Exploration of microbial Pb-tolerance and -removal capabilities has uncovered various mechanisms employed by these organisms. These include extracellular sequestration, alteration in cell morphology, efflux mechanism, precipitation, biosorption, intracellular Pb-bioaccumulation, and enhanced siderophore production (Naik and Dubey 2013; Chen et al. 2019). During bio-precipitation, an insoluble Pb-complex is formed which results in reduced bioavailability and toxicity. In the literature, examples of this mechanism include the production of insoluble Pb-phosphates (Levinson et al. 1996) and Pb-sulphides (De et al. 2008) by bacteria. During anaerobic respiration, inorganic compounds, such as nitrate or sulphate, can act as electron acceptors in the place of oxygen (aerobic respiration), yielding ammonium or nitrogen from nitrate (Simon and Klotz 2013) and sulphide ions from sulphate (Ophardt 2007). The potential for using sulfatesulphate-reducing bacteria to remove heavy metals from water has been investigated, especially where Pb is removed as a black precipitate in the form of immobile PbS (Niu et al. 2018).

Alternatively, soluble Pb(II) could be removed from water by reducing it to insoluble elemental Pb. Although in many cases the reduction in one metal species to a lower oxidation state is thermodynamically feasible in a broad redox range, a large activation energy is usually required to initiate the reaction. The required activation energy can, however, be reduced by the introduction of a catalyst to the system. In biological systems, enzymes act as catalysts and allow reactions usually requiring elevated temperatures to proceed at ambient temperatures (Karp 2010). This phenomenon was observed in the previous studies on the reduction in the toxic metals Cr(VI) to Cr(III) (Chirwa and Wang 1997, 2000; Bansal et al. 2019), U(VI) to U(IV) (Lovey et al. 1993; Mtimunye and Chirwa 2014, 2019) and Se(VI) or Se(IV) to Se(0) (NAMC 2010; Li et al. 2014; Tendenedzai and Brink 2019). In each case, microorganisms were discovered that facilitated the biotransformation of the metals to the lower oxidation state, despite the thermodynamic barriers. Often, the transformation is facilitated as part of a defence mechanism as the metal is converted to a less mobile state that cannot passively enter the cells (Haefeli et al. 1984; Kessi et al. 1999). In many species, energy for metabolism and cell growth is derived from the metal reduction process (Wade and DiChristina 2000). The total reduction of in metals to the zero valent state observed first in the reduction of divalent palladium to

the crystalline zero valent form by the cells of *Desulfovibrio desulfuricans* NCIMB 8307 (Lloyd et al. 1998; Yong et al. 2002), and more recently in the reduction of the tetravalent selenium oxyanions to zero valent selenium (NAMC 2010; Li et al. 2014; Tendenedzai and Brink 2019).

Owing to limitations faced by current technologies used for the removal of Pb(II) from aqueous media, methods for its extraction for direct reuse and removal from the anthropogenic cycle have proven elusive. The dissimilatory reduction of aqueous Pb(II) to elemental Pb would contribute significantly towards providing a biological method for Pb bio-recovery. However, currently limited investigations on the feasibility of biological reduction of Pb to the zero valent or crystalline state have been performed. Authors of the current study have published a number of papers showing promising results in terms of the microbial precipitation of Pb using industrially obtained microbial cultures; however, the identities of the precipitates formed were not determined (Brink et al. 2017; Brink and Mahlangu 2018; Peens et al. 2018; Hörstmann and Brink, 2019). The current research aimed to investigate the effects of oxygen on the effectiveness of microbial Pb-precipitation and precipitate identities.

The industrially sourced consortia were obtained from a borehole at an automotive battery recycling plant and a functioning Pb-mine. The consortia were cultivated in Pb-containing media under aerobic and anaerobic mesophilic conditions. The precipitates formed during fermentations were analysed to determine their exact chemical composition and thereby elucidate the precipitation mechanisms at work. The work was completed between April 2017 and June 2018 at the University of Pretoria, South Africa.

Materials and methods

Pb-resistant consortium screening and culture preparation

Soil samples were collected from a borehole at an automotive battery recycling plant in Gauteng, South Africa, and from the northern shaft of an operational Pb-mine in the Northern Cape Province, South Africa. The background Pb-concentrations in the soil were determined by leaching the soil using distilled water and concentrated HNO₃ to determine the Pb-concentration range of the soil, considering the pH dependence of the Pb-solubility. The Pb-concentrations were quantified using an atomic absorption spectrometer (PerkinElmer Analyst 400, Waltham, Massachusetts). The range of Pb-concentrations was determined to be between 3 and 150 ppm, based on the mass of soil.

The samples were screened for Pb-resistant organisms by suspending 1 g of soil in a sealed serum bottle (Sigma-Aldrich, St. Louis, MO) containing sterile fermentation medium consisting of standard Luria–Bertani (LB) broth (Merck, Darmstadt, Germany) and a background Pb-concentration of 80 mg L⁻¹. No attempt was made to purify or identify the consortium cultures; this would form part of a future project. The fermentation medium was prepared by blending separately sterilized LB broth and a 1000 mg L⁻¹ Pb (Merck, Darmstadt, Germany) stock solution. The cultures were cultivated anaerobically for 24 hours at 32 °C to ensure facultative anaerobic consortia. These cultures were dubbed B80 and N80 for the automotive battery recycling plant and mine cultures, respectively, to indicate the source of the consortia and the screening Pb-concentrations used.

Sterile glycerol was added to the balance of the cultures grown anaerobically for 24 h in order to obtain a final glycerol concentration of 20% v/v, from which 1 mL stock cultures were obtained and stored at -77 °C for further analysis.

All fermentations were inoculated from LB agar (Merck, Darmstadt, Germany) plates; prior to fermentations, 1 mL stock samples were thawed for 45 min in a 5 °C refrigerator. Sterile LB agar plates were streaked, sealed, and cultured for 24 h at 32 °C in an anaerobic atmosphere. After 24 h' growth, the plates were stored at 5 °C until required for fermentations.

Preparation of microbial cultures

Two loops of the plated bacteria were inoculated into the fermentation medium (see medium used for screening) for each of the triplicate experiments. In the anaerobic fermentations, the serum bottles were purged with nitrogen (Afrox, Johannesburg, South Africa) for three minutes and sealed with a rubber stopper, while the aerobic fermentations were performed in shaker flasks covered with sterile cotton wool.

Sampling and analysis

The sampling was performed by extracting approximately 6 mL samples from each of the triplicate batch reactors via a sterilised hypodermic needle. The samples were centrifuged for 10 min at 6000 rpm (Eppendorf® Minispin Z606235, Hamburg, Germany) and the effluent decanted and stored at 5 °C for further analysis. The pellet was re-suspended with distilled water, and the optical density at 600 nm (OD_{600}) and metabolic activity at 550 nm (MA) were measured spectrophotometrically (Lightwave II, WPA Labotech, South Africa) using the method described in Sect. 2.4.

An atomic absorption spectrometer (PerkinElmer AAnalyst 400, Waltham, Massachusetts) equipped with a Pb Lumina hollow cathode lamp (PerkinElmer AAnalyst 400, Waltham, Massachusetts) was used to measure the dissolved Pb-concentration in the centrifuge vial effluent.

Optical density and metabolic activity measurements

The metabolically active cells in the sample were quantified using the MTT method proposed by Wang et al. (2010). Water-insoluble formazan crystals are formed by the reduction in 3-(4,5-dimethylthiazol-2-yl)-2,5-diphenyl tetrazolium bromide (MTT) by the dehydrogenase system of viable cells in a culture. The formazan crystals are subsequently extracted using DMSO and spectrophotometrically quantifying at 550 nm providing a quantitative measure of the metabolic activity (MA) of the culture.

5 g L⁻¹ MTT solutions were prepared with MTT powder (Sigma-Aldrich, St. Louis, MO) and ultra-purified water, filtered with sterile filters into 2 ml cryogenic vials, placed in a dark container, and frozen at -40 °C until use.

For the optical density at 600 nm (OD_{600}) and MA analyses, 1 ml of the original samples taken from the bioreactors was diluted to a final volume of 4 ml, respectively. The OD_{600} was measured spectrophotometrically (Lightwave II, WPA Labotech, South Africa) to use as an indication of the biomass and amount of dark Pb-precipitate (Naik et al. 2013). No attempt was made to separate the biomass and precipitate as the MA was deemed to be a sufficient measure of the biocatalyst activity. Subsequently, 1.8 ml of the diluted samples was transferred to 2 ml cryogenic vials, and 0.2 ml of the prepared MTT, at room temperature, was added. The vials were sealed and incubated in darkness at 35 °C for 1 h. After the incubation was completed, the samples containing the formazan crystals were dissolved in 2 ml of DMSO (Sigma-Aldrich, USA) and mixed thoroughly. The absorbances of the vials at 550 nm were measured and recorded to quantify the MA (Lightwave II, WPA Labotech, South Africa).

For the OD_{600} and MA measurements without biomass, the same procedure was followed as described in the previous paragraph, after initially removing the biomass by centrifuging the sample (Universal 320 R, Hettich Zentrifugen, Germany) and filtering it with a 25-mm nylon syringe filter with 45 µm pores (Anatech). The net OD_{600} and MA were determined as the difference between the measurements with and without biomass. All results were reported after considering the dilution required to measure the values within the range of the instrument.

Pb-precipitate identification

The respective precipitate samples were qualitatively analysed by using a Zeiss Ultra PLUS FEG scanning electron microscope (SEM) coupled with energy-dispersive X-ray spectroscopy (EDX: Oxford instruments, Aztec software, 20 kV) (Naik et al. 2013). The samples selected for analysis were taken randomly from one of the triplicate vials at the termination of the experiment (144 h). Each precipitate sample was prepared by centrifuging two 1 mL collected samples at 9000 rpm for 10 min. The precipitate sample was then washed with a solution containing 50% v v⁻¹ ethanol and centrifuged at 9000 rpm for 10 min. The procedure was repeated with 60% v v⁻¹ ethanol, 80% v v⁻¹ ethanol, and twice with 100% ethanol, all at 9000 rpm for 10 min. The precipitate sample was then placed on a glass disc and left for 1 h to allow all ethanol to evaporate. The disc was placed on a metal stub, coated with gold and analysed with SEM-EDX. Ten different sites on each metal stub were analysed for each consortium's precipitate.

Subsequently, each precipitate sample was characterised by X-ray photoelectron spectroscopy (Thermo ESCALab 250 Xi, Waltham, MA) (Wang et al. 2004: 371). The samples were prepared anaerobically to ensure minimal oxidation of the precipitate during preparation. Two 1 mL collected samples were centrifuged at 9000 rpm for 10 min. The precipitate samples were dried anaerobically overnight in a sealed desiccator containing silica crystals, an AnaeroGen™ pouch (Oxoid Ltd, Basingstoke, UK), and an anaerobic indicator (Oxoid, Thermo Scientific, Basingstoke, Hampshire, UK), before being analysed with XPS.

Results and discussion

Visual difference between aerobic and anaerobic experiments

The observed differences between the aerobic (a and b) and anaerobic (c and d) conditions are demonstrated shown in Fig. 1. Based on visual evidence, significant differences in the final compositions are apparent, with a brown/yellow precipitate observed in the aerobic fermentations (a and b) and a dark precipitate observed in the anaerobic fermentations (c and d). The abiotic controls (e and f) displayed no visual change for either aerobic or anaerobic runs after 72 h, indicating that the precipitate formation was a result of biological activity of the consortia. The results from the anaerobic experiments are consistent with the anaerobic results obtained by Saiz and Barton (1992) as well as with other anaerobic work done by the authors of this paper (Brink and Mahlangu 2018; Peens et al. 2018; Brink et al. 2017) in which dark precipitates were observed. The results from the aerobic fermentations likely indicate the formation of a brown/yellow Pb-precipitate. It is known that Pb-oxide colours range from yellow (PbO), to red–orange (Pb₃O₄), and dark brown (PbO₂), providing a likely candidate for the precipitate as a Pb-oxide (Eastaugh et al. 2007:228). The results obtained for the aerobic precipitation experiment compare well with recently published work from Dabir et al. (2019) in which a brown discolouration was observed in an aerobic cultivation of an industrial consortia grown in LB broth media spiked with 400 ppm Pb(II).

Percent changes in dissolved Pb-concentrations (%Δ[Pb])

The measured %Δ[Pb] are shown in Fig. 2 with the data points representing the average percentage decline in the measured Pb-concentrations relative to the initial Pb-concentrations in the triplicate runs and the error bars indicating one standard deviation for results measured. The results indicate significant %Δ[Pb] exhibited for all the experimental runs, with total %Δ[Pb] of between 78.11 ± 4.02% and 88.76 ± 3.98% recorded after 144 h. The results for all the runs displayed similar trends with the majority of the %Δ[Pb] achieved within the first 48 h, in the range between 69.57 ± 2.84% and 76.61 ± 0.61% for all the runs, followed by a slower rate for the remainder of the runs.

The aerobic %Δ[Pb] for the B80 consortium were significantly faster than the corresponding run for the N80 consortium. The B80 run achieved a fast %Δ[Pb] of 71.38 ± 5.71% within the first 24 h, when compared to the N80%Δ[Pb] of 19.35 ± 1.36% within the same period. The period between 24 and 48 h showed a marked decline in the rate of %Δ[Pb] in the aerobic B80 with a measured value of 76.61 ± 0.61% when compared to the aerobic N80%Δ[Pb] for the same period which rapidly increased to 69.57 ± 2.84%. It is interesting that the %Δ[Pb] in the aerobic N80 decreased to 66.50 ± 1.04% within the period from 48 to 72 h, implying a release of Pb(II) ions back into the solution. This might indicate an initial adsorption–desorption mechanism present in the N80 consortium. Microbial biomass obtained from activated sludge is reported to provide good sorption sites for

	0 h	24 h	48 h	72 h	144 h
B80 Aerobic					
N80 Aerobic					
B80 Anaerobic					
N80 Anaerobic					
Aerobic Control					
Anaerobic control					

Fig. 1. Images showing the fermentation vials for the aerobic and anaerobic experiments as well as the corresponding abiotic control experiments— aerobic and anaerobic. The figure shows the timescale from initiation of the experiments to completion at 144 h

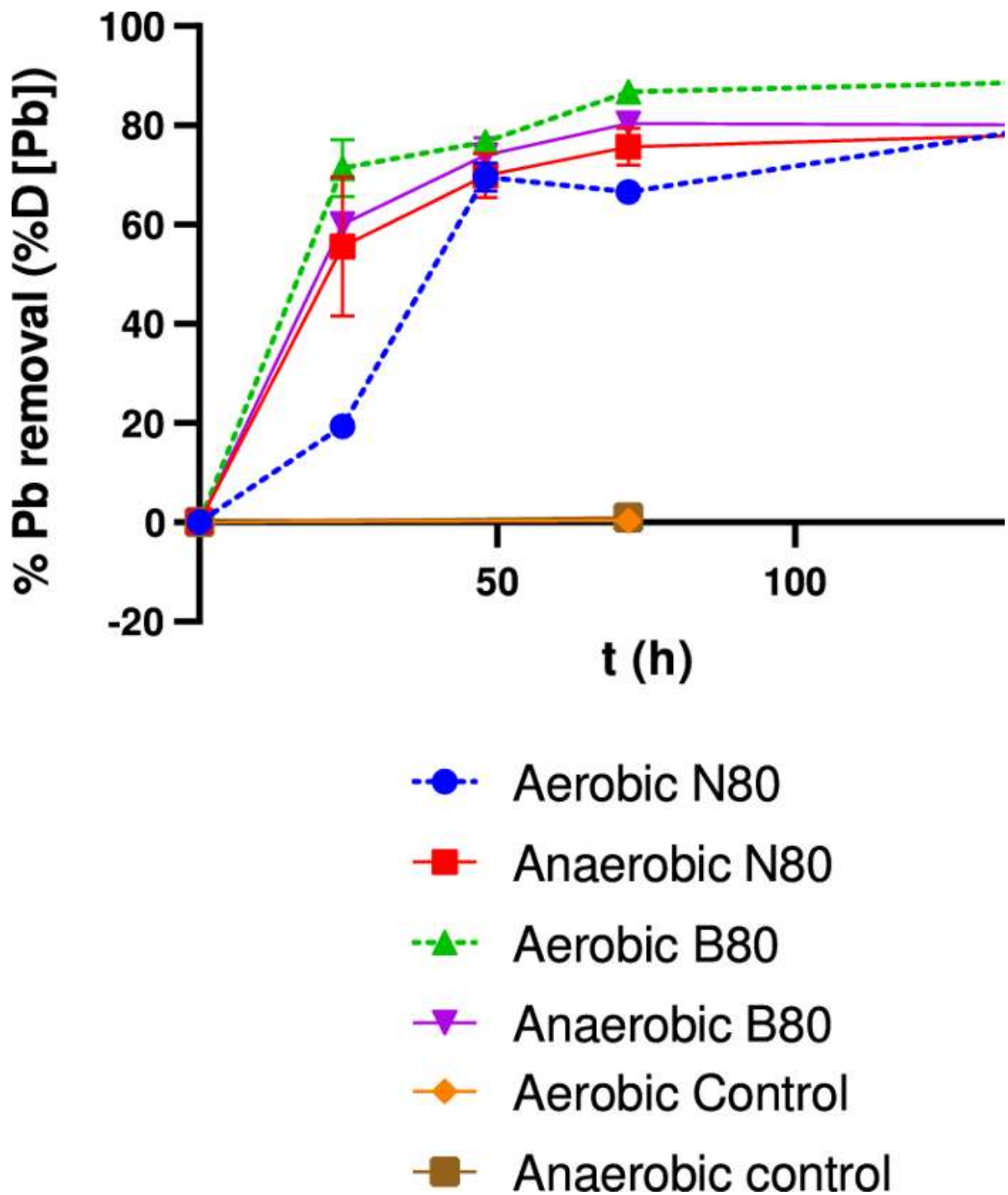


Fig. 2. % Δ [Pb] graphs for the aerobic and the anaerobic runs. The data points represent the average, and error bars indicate the standard deviation for the triplicate experiments

Pb (Adeniji 2004; Chatterjee et al. 2012; Singh et al. 2014). It should be noted that the medium in the aerobic B80 run became yellow/brown after 24 h, in contrast to the aerobic N80 that started to turn yellow/brown between 48 and 72 h.

The anaerobic results, shown in Fig. 2, display a clear and significant increase in $\% \Delta[\text{Pb}]$ over time. Findings suggest no significant differences between $\% \Delta[\text{Pb}]$ attained by the respective consortia under anaerobic conditions when considering the distribution of the data, perhaps indicating that similar strains of organisms were active (i.e. able to remove Pb(II)) under the relevant conditions. This is a distinct possibility given the anaerobic conditions with high background Pb-concentrations that might favour a limited subset of organisms, specifically those capable of removing Pb(II) ions.

The $\% \Delta[\text{Pb}]$ results obtained for the experiments compare well with the published literature. Dabir et al. (2019) reported Pb(II) removals of between 39 and 58% after 72 h of a 400 ppm solution inoculated with industrial consortia. Kafilzadeh et al. (2012) measured Pb(II) removals of between 60 and 90% in 11 h of an initial Pb(II) concentration of 450 ppm by various industrially isolated bacteria. Verma et al. (2017) observed a 98% removal of 80 ppm Pb(II) in 7 days by a sulphate-reducing consortium, and Kang et al. (2015) reported a 68% removal of 7 ppm Pb(II) from solution in 48 h by *Enterobacter cloacae*.

Optical density (OD_{600}) and metabolic activity (MA) measurements

Figure 3 shows the measured optical density of light at 600 nm (OD_{600}) (a and b) as well as the metabolic activity in the reactors at 550 nm (MA) as measured by the MTT method (see Sect. 2.4) (c and d), for all the runs. The OD_{600} results (Figure Fig. 3a, b) demonstrate that a significant difference in the aerobic B80 and N80 cultures was observed. The OD_{600} for the aerobic B80 cultures increased to 11.30 ± 0.85 absorbance units (a.u.) within the first 48 h, before decreasing to 9.25 ± 0.09 a.u. during the remainder of the fermentations. In contrast, the results from the aerobic N80 culture exhibited a lag period until at least 24 h before increasing to 4.23 ± 1.15 after 48 h and 6.70 ± 0.09 a.u. after 72 h. These results mirror the corresponding visual results shown in Fig. 1a, b for the aerobic conditions in the B80 versus N80 runs in which it can be seen that the growth for the N80 aerobic runs appeared less dense than the B80 aerobic run at the same experimental time.

The MA results (Fig. 3c, d) display a substantial increase in the MA for the aerobic B80 in the first 48 h, with an increase to 16.34 ± 0.77 a.u. within the first 24 h, followed by an increase to 62.42 ± 6.66 a.u. at 48 h. In the period between 48 h and 72 h, the aerobic B80 MA collapsed to 7.66 ± 0.27 a.u., remaining relatively constant for the remainder of the experiment with a final MA of 5.42 ± 0.19 a.u. measured after 144 h. In comparison, the aerobic N80 MA remained nearly constant at a value of 0.31 ± 0.06 a.u. for the initial 24 h; this was followed by an increase to 4.53 ± 1.15 a.u. after 48 h before remaining relatively constant for the remainder of the experiment with a final MA of 3.56 ± 0.12 a.u. after 144 h. It is notable that after 48 h, the aerobic B80 consortium was 13 times more metabolically active than the aerobic N80 culture, while only a modestly better $\% \Delta[\text{Pb}]$ of $76.6 \pm 0.61\%$ in the aerobic B80 culture was achieved as compared to $69.57 \pm 2.84\%$ in the aerobic N80 culture. The results hint at different microbial fractions with significantly varied metabolic characteristics present in the B80 culture. First, there appeared to be a highly active aerobic microbial fraction of the B80 consortium, which grew at a remarkable speed within the first 48 h before perishing, likely because of starvation. This fraction had limited impact on the Pb(II) removal. Second, a less active fraction, which grew more slowly than the first, was responsible for the removal of Pb(II)-ions from solution.

In both anaerobic cultures, most of the change in OD_{600} and MA took place within the initial 24 h; similar OD_{600} values of 3.67 ± 0.03 a.u. and 3.27 ± 0.29 a.u., and MA values of 6.03 ± 0.14 a.u. and 5.06 ± 0.17 were measured in the anaerobic B80 and N80 cultures, respectively. This was followed by a slight divergence of the two OD_{600} curves; the B80 OD_{600} and MA remained nearly constant at an OD_{600} of 3.78 ± 0.19 a.u. and 5.38 ± 0.33 a.u. after 144 h. The anaerobic N80 culture dropped below the anaerobic B80 curve in the period from 24 h to 48 h resulting in an OD_{600} of 2.75 ± 0.30 a.u. and MA of 3.84 ± 0.21 a.u. after 48 h. The latter OD_{600} and MA subsequently remained nearly constant for the remainder of the experiment resulting in final readings of 2.61 ± 0.23 and 3.22 ± 0.31 a.u. after 144 h.

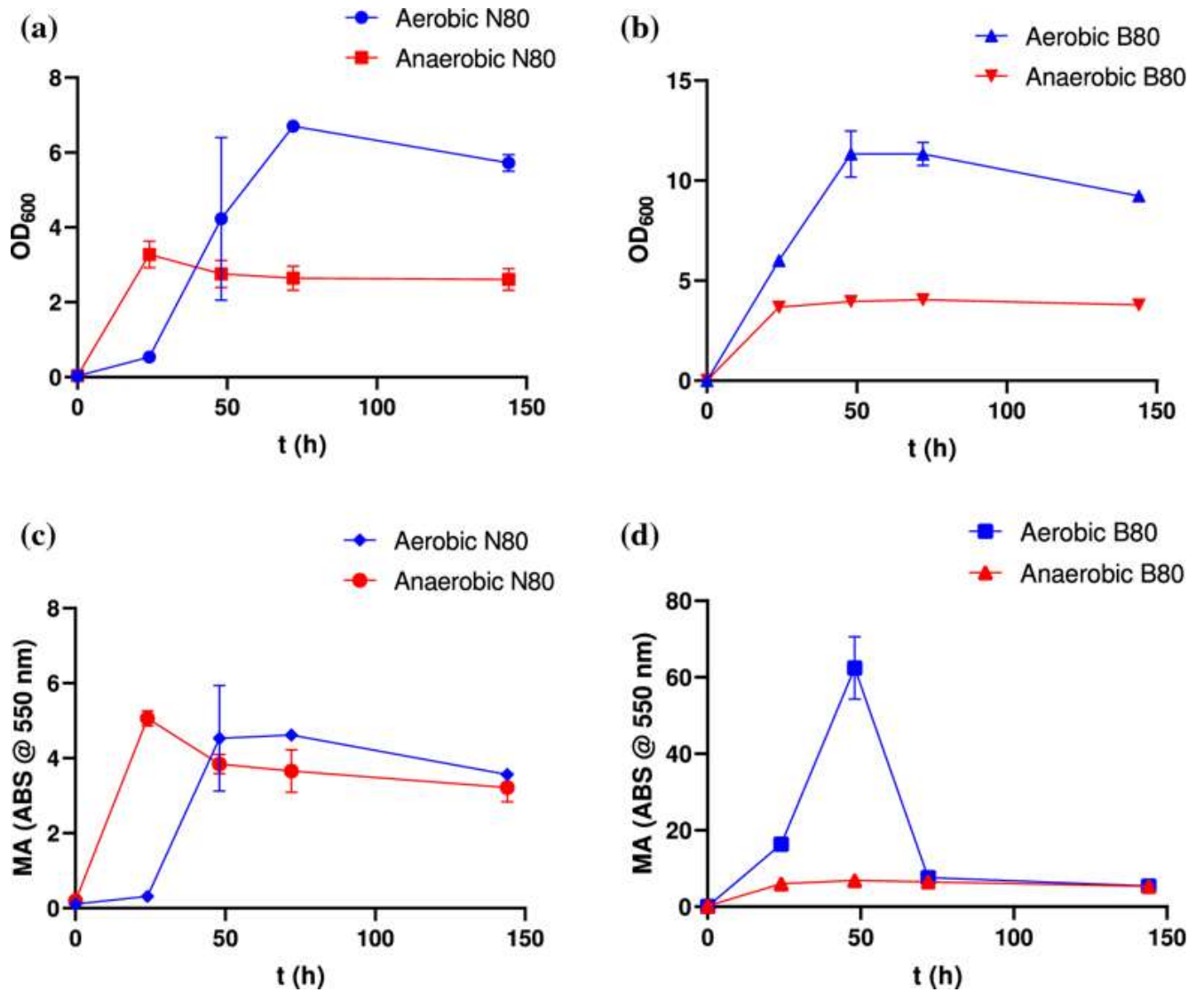


Fig. 3. OD₆₀₀ of the **a** N80 an, **b** B80 graphs and the MA of the **c** N80 and **d** B80 runs for the aerobic and the anaerobic runs. The data points represent the average, and error bars reflect the standard deviation for the triplicate experiments

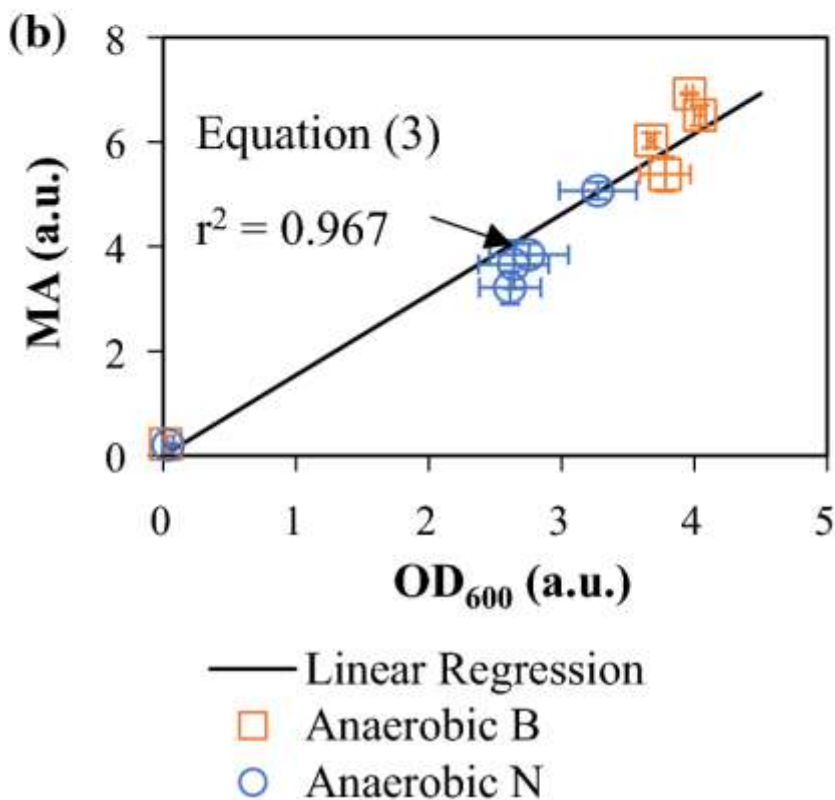
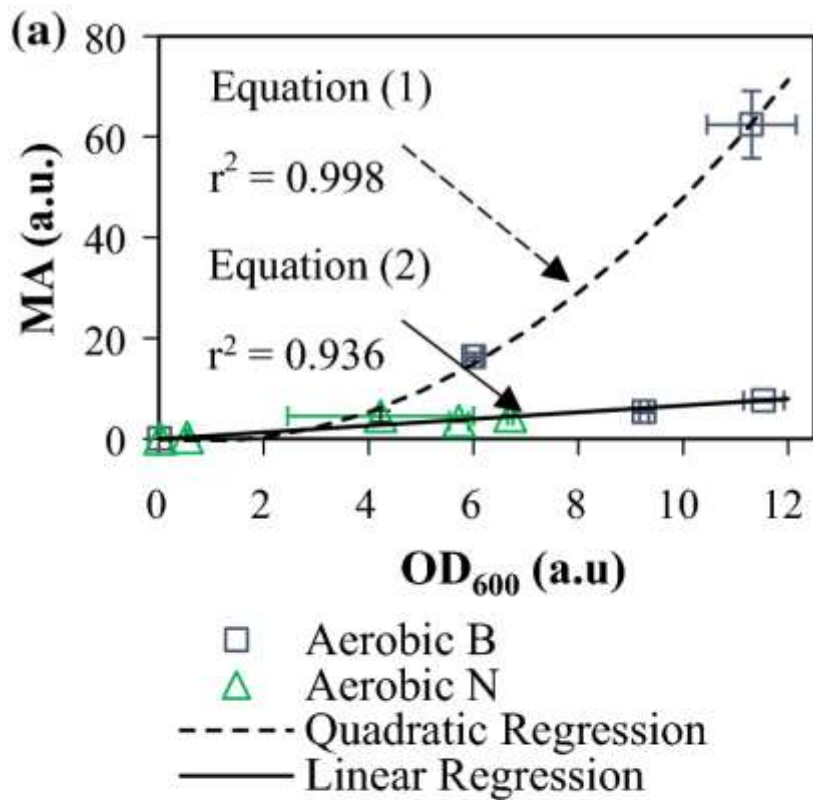


Fig. 4. Correlation between the OD₆₀₀ and MA results obtained for the **a** aerobic runs and **b** anaerobic runs. The relationships described by Eqs. (1) to (3) as well as the respective coefficients of determination are plotted in the figures and indicated with arrows. The data points represent the average values and error bars indicate the standard deviation for the triplicate experiments

The overall MA results showed similar values for all the runs after 72 h that were maintained for the remainder of the experiments. This is remarkable considering the substantial increase in the MA in the aerobic B80 culture within the initial 48 h. This observation, coupled with the observation that similar Pb(II) removal trends were observed for all the runs, indicates similarities between the fractions of the consortia responsible for Pb(II) removal. Figure 4 shows the correlations between corresponding OD₆₀₀ and MA values measured for the aerobic (a) and anaerobic (b) conditions. The results from the aerobic B80 and N80 runs were described by two different correlations, a quadratic fit defined by Eq. (1) with a coefficient of determination (r^2) of 0.998, and a linear fit defined by Eq. (2) with an $r^2 = 0.936$.

$$MA = 0.576(OD_{600})^2 - 0.976(OD_{600}) \quad (1)$$

$$MA = 0.665 (OD_{600}) \quad (2)$$

In addition, a strong correlation was observed between the OD₆₀₀ and MA values for the anaerobic B80 and N80 results. The combined results from the anaerobic B80 and N80 runs are well-described by a linear regression (Eq. 3) with an $r^2 = 0.967$.

$$MA = 1.539 (OD_{600}) \quad (3)$$

These results support the hypothesis that the B80 consortium consisted of different population fractions with dissimilar metabolic activities. The fast-growing fraction of the aerobic B80 showed a nonlinear increasing MA per OD₅₅₀ described by a quadratic function. This likely indicates an increased activity per biomass dry weight as a result of a higher enzyme concentration per mass of microbial cells during the fast growth section, assuming the OD₆₀₀ is directly proportional to the mass of biomass in the system. Nannipieri et al. (1983) reported a significant increase in microbial enzyme activity in response to the addition of energy sources, while Rinkes et al. (2014) reported an increase in activity per mass of an aerobic microbial consortium over time. In this study, the aerobic environment would provide increased ATP production to the aerobic B80 fraction through oxidative phosphorylation in the metabolism resulting in increased biomass production. In contrast, the results from the slow-growing fraction of the aerobic B80 consortium combined with the results from the aerobic N80 fraction follow a linear relationship with biomass concentration. This relationship is described by Eq. (3) and indicates a constant activity per mass of microbial cells. The same observation can be made about the linear relationship between the MA and OD₅₅₀ in the anaerobic B80 and N80 runs.

These results further indicate an increased activity in Pb-active biomass present under anaerobic conditions when compared to aerobic conditions; the MA per OD₆₀₀ in the aerobic conditions are significantly greater than in the anaerobic conditions, a slope of 1.539 versus 0.665 for the anaerobic versus aerobic correlations (Eqs. 2, 3). This phenomenon is likely a result of starvation conditions experienced by the Pb-active biomass under aerobic conditions due to competition for resources with the fast-growing aerobic biomass. This competition for resources would be absent under anaerobic conditions therefore promoting greater meta-

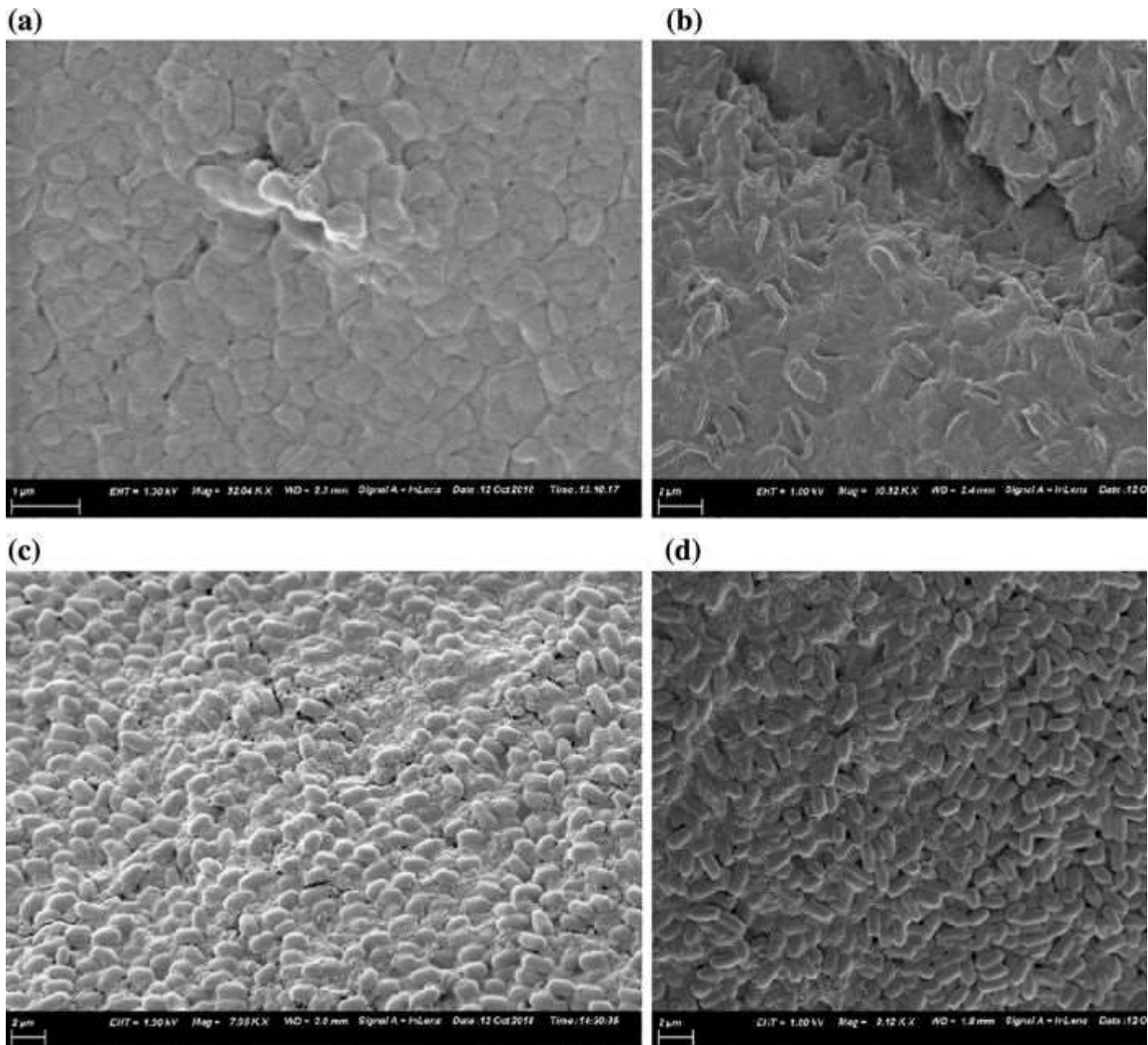


Fig. 5. SEM micrographs of the precipitate and bacteria for the **a** aerobic B80, **b** aerobic N80, **c** anaerobic B80, and **d** anaerobic N80 runs. The scale bar for the respective micrographs are indicated in the bottom right

bolic activity of the Pb-active biomass.

SEM-EDX and XPS

The SEM micrographs presented in Fig. 5 show significant differences in the observed solid fractions formed in the respective runs. The micrograph of the aerobic B80 run (a) supports the hypothesis of cellular death with nearly no microbial cells apparent and only precipitate observed. The shape of the precipitate points to the remains of microbial cells buried under the surface. EDX confirmed the presence of significant fractions of Pb within the precipitate, with atomic percentages of between $0.42 \pm 0.01\%$ and $3.56 \pm 0.93\%$. The sample preparation for the SEM micrographs involved multiple washing steps that would likely have removed any adsorbed Pb(II) from the surface of the cells, and therefore it can be concluded that the micrographs do not represent adsorbed Pb(II) but rather Pb-precipitates. The aerobic N80 micrograph (b) also shows the remains of ruptured microbial cells, specifically when the shapes are compared to the anaerobic micrographs (c) and (d). The cellular remains appear imbedded in the precipitate matrix. In contrast, the micrographs for both anaerobic cultures appear to show viable bacilli of approximately 1–2 μm in length and 0.5–1 μm in diameter. These results mirror the MA and OD₆₀₀ results which saw constant values measured until the termination of the experiments after 144 h, an indication of maintained viability in comparison with the reduction in MA and OD₅₅₀ in the aerobic runs.

Both consortial precipitates showed that the microbial cultures were imbedded in the precipitate structure, suggesting that the precipitation took place on the surface of the microbes as opposed to the precipitate being excreted from the microbes. This suggests an external precipitation mechanism as opposed to an internal mechanism coupled with an excretion mechanism. Potentially, a surface electron transfer mechanism could be active for direct Pb(II) reduction similar to that proposed by Mtimunye and Chirwa (2014) for the microbial reduction in U(VI) to U(IV). Alternatively, or additionally, sulphur-containing amino - acids could be metabolised intracellularly, coupled with the excretion of sulphide to the medium which would then precipitate PbS on contact with dissolved Pb(II) in the medium. Loiseau et al. (2003) found evidence of a microbial cysteine desulphurase responsible for the biogenesis of FeS by the desulphurisation of cysteine to alanine which can in turn enter the TCA-cycle via pyruvate as a carbon source.

The XPS profiles for Pb-identification are presented in Fig. 6. The relative abundance of the Pb-species present in the precipitates are is reported in Table 1. The XPS results provide interesting insight into the mechanism of Pb-precipitate formation present in the different consortia for the aerobic and anaerobic conditions. The aerobic B80 and N80 XPS results show that the Pb-precipitate presented exclusively as PbO and elemental Pb. This observation is corroborated by the observed colour of the precipitate being yellow/brown. In comparison, the anaerobic B80 and N80 results indicated significant fractions of PbS present in the precipitate, likely a result of the liberation of S²⁻-ions during the catabolism of sulphur-containing cysteine and methionine by the organism.

Table 1 XPS results showing the relative abundance of Pb-species present in the precipitates obtained from the aerobic and anaerobic B80 and N80 cultures

Consortium	Conditions	PbO (%)	Pb ⁰ (%)	PbS (%)	
B80	Aerobic	89	11	0	
	Anaerobic	38	38	54	
N80	Aerobic	79	21	0	

The lack of PbS in the aerobic runs can possibly be attributed to the oxidation of any S^{2-} -ions intracellularly prior to excretion. The lack of $PbSO_4$ or $PbSO_3$ precipitates is likely a result of the difference in the solubility products of PbS (3.2×10^{-28}), $PbSO_4$ (1.8×10^{-8}), and $PbSO_3$ (2.5×10^{-8}), which resulted in significantly lower precipitation of $PbSO_4$ observed. The differences in solubility products translate

to a maximum SO_4^{2-} concentration of 4.47 mg L^{-1} and SO_3^{2-} of 5.18 mg L^{-1} before precipitation is observed as compared to $2.00 \times 10^{-20} \text{ mg L}^{-1} S^{2-}$. Alternatively, aerobic conditions inhibited the metabolism of sulphur-containing amino-acids and consequently suppressed the formation of sulphur species in solution. The difference in sulphur presence between the anaerobic and aerobic runs requires further investigation.

The balance of the Pb-precipitates in all the runs was a combination of PbO and PbO. The hypothesis is that the measured PbO is due to the oxidation of elemental Pb in the aerobic runs or as a result of oxygen exposure during sample preparation in the anaerobic runs. The main motivation for this argument hinges on the presence of exclusively PbS, PbO, and elemental Pb. The oxidation of PbS to PbO at intermediate temperatures leads to a partial oxidation of PbS to PbO and $PbSO_4$; for complete oxidation of PbS to PbO to occur, temperatures in excess of $800 \text{ }^\circ\text{C}$ are required (Abdel-Rehim 2006). This means that the PbO was produced independently from the PbS. Additionally, no precipitate was observed in abiotic aerobic and anaerobic control experiments (Fig. 1e, f), indicating that the Pb(II) did not chemically react with oxygen to produce PbO. Therefore, the presence of PbO could not be attributed to the presence of oxygen in the aerobic system and by extension excludes oxidation as a result of trace amounts of oxygen in the anaerobic experiments. It is more likely that the PbO was formed either directly by the microbial action in the system or because of the oxidation of elemental Pb during the aerobic runs or during processing of the precipitate for XPS analysis.

Elemental Pb oxidises spontaneously in normal atmosphere to form a layer of PbO; the overall redox reaction $2Pb + O_2 \rightarrow 2PbO$ has $\Delta G < 0$ (Hitchman et al. 1997). In this system, the formation of PbO from Pb(II) would require a source of oxygen, most likely from H_2O . This would result in an increase in H^+ ions and a subsequent decrease in pH. The final pH for all anaerobic fermentations involving these consortia were previously reported to be in the range of 5.5-6.5 (Brink et al. 2017; Brink and Mahlangu 2018; Peens et al. 2018); this scenario is therefore unlikely. It is concluded that the precipitate formed under aerobic conditions by the microbial species was initially exclusively elemental Pb, and under anaerobic conditions consisted of a mixture of PbS and elemental Pb.

The researchers hypothesise that the microbial production of Pb-precipitate under aerobic conditions is related to an oxidation-reduction mechanism, while under anaerobic precipitation, it is related to a combination of an oxidation-reduction mechanism and a sulphide-liberation mechanism through the catabolism of the sulphur-containing amino acids cysteine and methionine. This implies that the Pb(II) initially loaded into the batch

reactors acted as an electron acceptor in all cases. Carbon sources would be oxidised to CO_2 during catabolism, releasing a number of electrons which, in turn, reduced the Pb(II) to elemental Pb-precipitate. Significantly, the precipitate formed has the potential to recover lead from processing plant and mine tailings waste streams as it can be recycled and processed together with the mined galena during Pb-smelting

(Shamsuddin 2016). From a thermodynamic perspective, the reduction of Pb(II) requires free energy ($\Delta G_{R'} = 12.4 \text{ kJ (mol e}^{-})^{-1}$ transferred) (Vanýsek 2011:8-23), while the oxidation of proteins (amino acids) provides free energy for the organism ($\Delta G_{R'} = -32.2 \text{ kJ (mol e}^{-})^{-1}$ transferred) (Kienzler and Swanson 2017:10) resulting in a net free energy of $\Delta G_{R'} = -19.8 \text{ kJ (mol e}^{-})^{-1}$ transferred. $\Delta G_{R'}$ describes the Gibbs free energy of the oxidation-reduction half-reaction at a pH of 7, temperature of $25 \text{ }^\circ\text{C}$, and activities of the species of 1 M. In comparison, the reduction of oxygen provides large amounts of free energy to the system ($\Delta G_{R'} = -29.5 \text{ kJ (mol e}^{-})^{-1}$ transferred) (Vanýsek 2011:8-23), therefore favouring the aerobic metabolism as a source of energy due to the large net energy $\Delta G_{R'} = -41.9 \text{ kJ (mol e}^{-})^{-1}$ transferred.

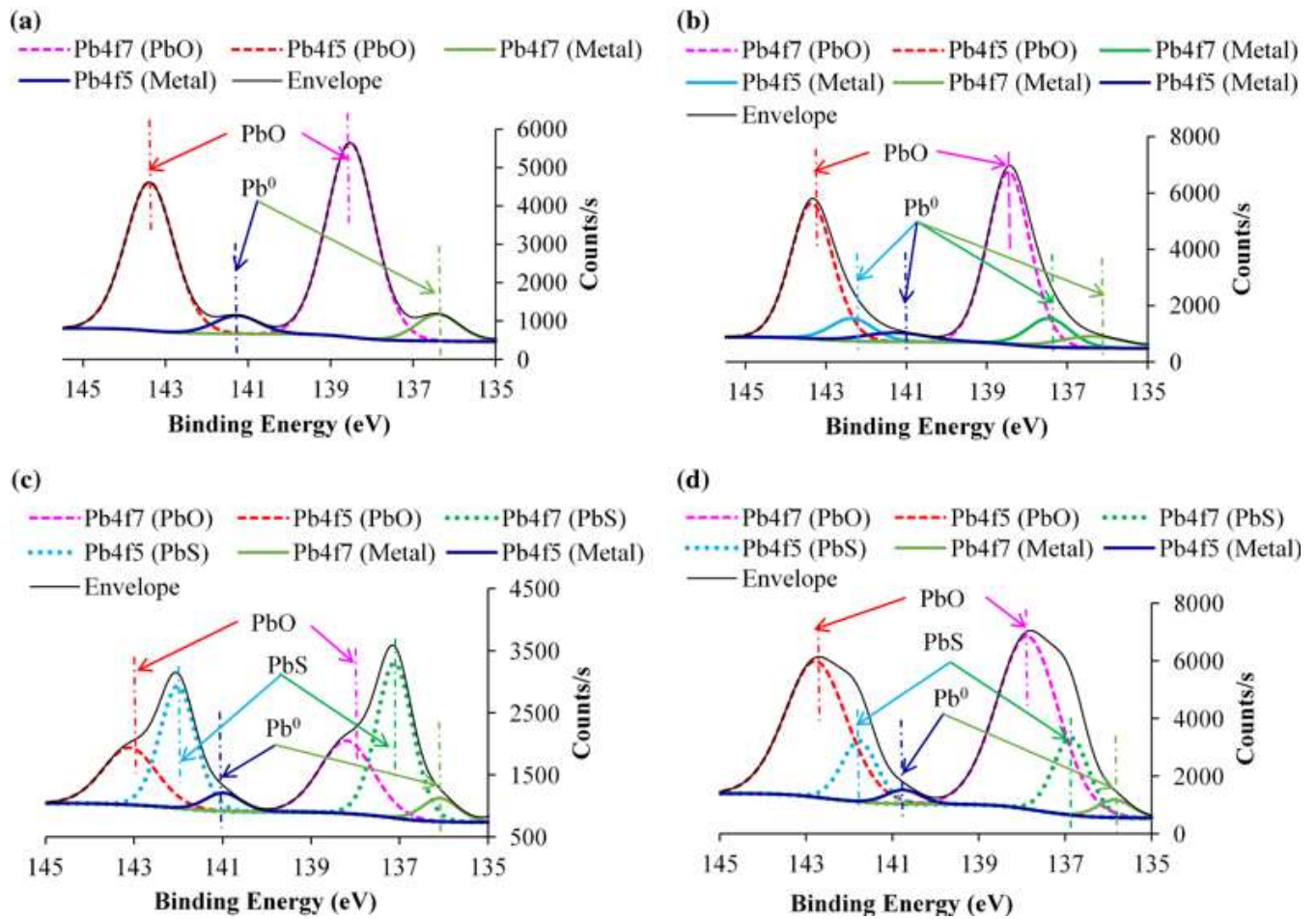


Fig. 6. XPS profiles of Pb-species for the **a** aerobic B80, **b** aerobic N80, **c** anaerobic B80, and **d** anaerobic N80. The peaks at 137.6 eV and 142.5 eV in (b) were identified as secondary Pb⁰-peaks as opposed to PbS or PbO₂, due to the absence of sulphide and PbO₂-specific oxygen peaks in the XPS profiles for sulphur and oxygen (not shown)

Conclusion

Results indicate that the consortia obtained from the mine and the recycling plant behaved comparably during Pb-precipitation experiments under corresponding aeration conditions, with similar Pb-removal capabilities of the consortia observed. Similarities are attributed to the high Pb-content in the reactors and the scarcity of organisms capable of thriving under such conditions. However, significant differences between the consortia were observed with respect to growth and metabolic activities under aerobic conditions; the B80 consortium displayed substantially greater growth and metabolic activities when compared to the N80 consortium. These differences were attributed to a mixed culture with dissimilar activities and growth behaviour exacerbated by the presence of oxygen under aerobic conditions. The precipitate identities were confirmed by XPS analysis to be mostly elemental Pb which spontaneously oxidised to PbO in the aerobic runs, while mostly PbS combined with elemental Pb was observed in the anaerobic runs.

This study provides the first evidence of bacterial dissimilatory reduction of Pb(II) to elemental lead in the literature. It is hypothesised that the precipitation of the Pb involves an oxidation–reduction mechanism in which the Pb(II) in the growth media acts as an electron acceptor. Under anaerobic conditions this mechanism was linked to the liberation of sulphide ions by the catabolism of sulphur-containing amino acids, which resulted in the precipitation of PbS and elemental Pb. The high-percentage Pb-removal (in excess of 78% for all the runs) indicates a promising concept for the immobilisation and possible recovery of Pb from contaminated water sources, including industrial waste streams, rivers, and groundwater sources.

Acknowledgements

This work is based on the research supported in part by the National Research Foundation of South Africa for the Grant, Unique Grant No. 106938.

Compliance with ethical standards

Conflict of interest

The authors declare that they have no conflict of interest.

References

- Abdel-Rehim AM (2006) Thermal and XRD Analysis of Egyptian Galena. *J Therm Anal Calorim* . 86:393–401. <https://doi.org/10.1007/s10973-005-6785-6>
- Adeniji A (2004) Bioremediation of Arsenic, Chromium, Lead and Mercury, EPA Report. Washington, DC.
- Aziz HA, Adlan MN, Ariffin KS (2008) Heavy metals (Cd, Pb, Zn, Ni, Cu and Cr(III)) removal from water in Malaysia: post treatment by high quality limestone. *Bioresour Technol* 99:1578–1583. <https://doi.org/10.1016/j.biortech.2007.04.007>
- Bansal N, Coetzee JJ, Chirwa EMN (2019) In situ bioremediation of hexavalent chromium in presence of iron by dried sludge bacteria exposed to high chromium concentration. *Ecotoxicol Environ Saf* 172:281–289. <https://doi.org/10.1016/j.ecoenv.2019.01.094>
- Barakat MA (2011) New trends in removing heavy metals from industrial wastewater. *Arab J Chem* . 4:361–377. <https://doi.org/10.1016/j.arabjc.2010.07.019>
- Barbaro P, Liguori F (2009) Ion exchange resins: catalyst recovery and recycle. *Chem Rev* 109:515–529. <https://doi.org/10.1021/cr800404j>
- Barbosa F, Fillion M, Lemire M, Sousa Passos CJ, Lisboa Rodrigues J, Philibert A, Guimarães JR, Mergler D (2009) Elevated blood lead levels in a riverside population in the Brazilian Amazon. *Environ Res* 109:594–599. <https://doi.org/10.1016/j.envres.2009.03.005>

- Block C, Dams R (1975) Lead contents of coal, coal ash and fly ash. *Water Air Soil Pollut* . 5:207–211
- Bollhöfer A, Rosman KJR (2000) Isotopic source signatures for atmospheric lead: the Southern Hemisphere. *Geochim Cosmochim Acta* 64:3251–3262. [https://doi.org/10.1016/S0016-7037\(00\)00630-X](https://doi.org/10.1016/S0016-7037(00)00630-X)
- Brink HG, Mahlangu Z (2018) Microbial Lead(II) precipitation: the influence of growth substrate. *Chem Eng Trans* 64:439–444. <https://doi.org/10.3303/CET1864074>
- Brink HG, Lategan M, Naudé K, Chirwa EMN (2017) Lead removal using industrially sourced consortia: influence of lead and glucose concentrations. *Chem Eng Trans* 57:409–414. <https://doi.org/10.3303/CET1757069>
- Chatterjee S, Mukherjee A, Sarkar A, Roy P (2012) Bioremediation of lead by lead-resistant microorganisms, isolated from industrial sample. *Adv Biosci Biotechnol* 3:290–295. <https://doi.org/10.4236/abb.2012.33041>
- Chen H, Xu J, Tan W, Fang L (2019) Lead binding to wild metal-resistant bacteria analyzed by ITC and XAFS spectroscopy. *Environ Pollut* 250:118–126. <https://doi.org/10.1016/j.envpol.2019.03.123>
- Chirwa EMN, Wang YT (1997) Hexavalent chromium reduction by *Bacillus* sp. in a packed-bed bioreactor. *Environ Sci Technol* 31:1446–1451. <https://doi.org/10.1021/es9606900>
- Chirwa EMN, Wang YT (2000) Simultaneous chromium(VI) reduction and phenol degradation in an anaerobic consortium of bacteria. *Water Res* 34:2376–2384. [https://doi.org/10.1016/S0043-1354\(99\)00363-2](https://doi.org/10.1016/S0043-1354(99)00363-2)
- Dabir A, Heidari P, Ghorbani H, Ebrahimi A (2019) Cadmium and lead removal by new bacterial isolates from coal and aluminum mines. *Int J Environ Sci Technol*. <https://doi.org/10.1007/s13762-019-02303-9>
- Eastaugh N, Walsh V, Chaplin T, Siddall R (2007) *Pigment compendium: a dictionary of historical pigments*. Taylor & Francis, Abingdon-on-Thames
- Eisler R (1988) Lead hazards to fish, wildlife and invertebrates: a synoptic review. *Biol Rep* 85:1–94. <https://doi.org/10.5962/bhl.title.11357>
- Gioia SMCL, Pimentel MM, Tessler M, Dantas EL, Campos JEG, Guimarães EM, Maruoka MTS, Nascimento ELC (2006) Sources of anthropogenic lead in sediments from an artificial lake in Brasília-central Brazil. *Sci Total Environ* 356:125–142. <https://doi.org/10.1016/j.scitotenv.2005.02.041>
- Haefeli C, Franklin C, Hardy K (1984) Plasmid-determined silver resistance in *Pseudomonas stutzeri* isolated from a silver mine. *J Bacteriol* 158:389–392
- Hitchman ML, Cade NJ, Gibbs TK, Hedley NJM (1997) Study of the factors affecting mass transport in electrochemical gas sensors. *Analyst* 122:1411–1417. <https://doi.org/10.1039/a703644b>
- Hörstmann C, Brink HG (2019) Microbial lead (II) precipitation: the influence of aqueous Zn (II) and Cu (II). *Chem Eng Trans* 74:1447–1452. <https://doi.org/10.3303/CET1974242>
- International Lead Association (2018) Lead production & statistics. <https://www.ila-lead.org/lead-facts/lead-production-statistics>. Accessed 5 Aug 2018
- Kafilzadeh F, Afrough R, Johari H, Tahery Y (2012) Range determination for resistance/tolerance and growth kinetic of indigenous bacteria isolated from lead contaminated soils near gas stations (Iran). *Eur J Exp Biol* 2(1):62–69
- Karp G (2010) *Cell and molecular biology: concepts and experiments*, 6th edn. John Wiley & Sons Inc, Hoboken
- Kessi J, Ramuz M, Wehrli E, Spycher M (1999) Reduction of selenite and detoxification of elemental selenium by the phototrophic bacterium *Rhodospirillum rubrum*. *Appl Environ Microbiol* 65:4734–4740
- Kienzler B, Swanson JS (2017) *Microbial effects in the context of past german safety cases*. KIT Scientific Publishing, Karlsruhe

- Levinson HS, Mahler I, Blackwelder P, Hood T (1996) Lead resistance and sensitivity in *Staphylococcus aureus*. *FEMS Microbiol Lett* 145:421–425. <https://doi.org/10.1111/j.1574-6968.1996.tb08610.x>
- Lloyd JR, Yong P, Macaskie LE (1998) Enzymatic recovery of elemental palladium by using sulfate-reducing bacteria. *Appl Environ Microbiol* . 64:4607–4609
- Loiseau L, Ollagnier-de-Choudens S, Nachin L, Fontecave M, Barras F (2003) Biogenesis of Fe-S cluster by the bacterial suf system. SufS and SufE form a new type of cysteine desulfurase. *J Biol Chem* 278:38352–38359. <https://doi.org/10.1074/jbc.M305953200>
- Lovley DR, Roden EE, Phillips EJP, Woodward JC (1993) Enzymatic iron and uranium reduction by sulfate-reducing bacteria. *Mar Geol* 113:41–53. [https://doi.org/10.1016/0025-3227\(93\)90148-O](https://doi.org/10.1016/0025-3227(93)90148-O)
- Manzoor M, Gul I, Ahmed I et al (2019) Metal tolerant bacteria enhanced phytoextraction of lead by two accumulator ornamental species. *Chemosphere* 227:561–569. <https://doi.org/10.1016/j.chemosphere.2019.04.093>
- Mathee A (2014) Towards the prevention of lead exposure in South Africa: contemporary and emerging challenges. *Neurotoxicology* 45:220–223. <https://doi.org/10.1016/j.neuro.2014.07.007>
- Mathee A, Khan T, Naicker N, Kootbodien T, Naidoo S, Becker P (2013) Lead exposure in young school children in South African subsistence fishing communities. *Environ Res* 126:179–183. <https://doi.org/10.1016/j.envres.2013.05.009>
- Mathee A Naicker N, Teare J (2015) Retrospective investigation of a lead poisoning outbreak from the consumption of an ayurvedic medicine: Durban, South Africa. *Int J Environ Res Public Health* 12:7804–7813. <https://doi.org/10.3390/ijerph120707804>
- Mtimunye PJ, Chirwa EMN (2014) Characterization of the biochemical-pathway of uranium (VI) reduction in facultative anaerobic bacteria. *Chemosphere* 113:22–29. <https://doi.org/10.1016/j.chemosphere.2014.03.105>
- Mtimunye PJ, Chirwa EMN (2019) Uranium (VI) reduction in a fixed-film reactor by a bacterial consortium isolated from uranium mining tailing heaps. *Biochem Eng J* 145:62–73. <https://doi.org/10.1016/j.bej.2019.02.002>
- Naik MM, Dubey SK (2013) Lead resistant bacteria: lead resistance mechanisms, their applications in lead bioremediation and biomonitoring. *Ecotoxicol Environ Saf* 98:1–7. <https://doi.org/10.1016/j.ecoenv.2013.09.039>
- Naik MM, Khanolkar D, Dubey SK (2013) Lead-resistant *Providencia alcalifaciens* strain 2EA bioprecipitates Pb⁺² as lead phosphate. *Lett Appl Microbiol* 56:99–104. <https://doi.org/10.1111/lam.12026>
- NAMC (2010) Review of available technologies for the removal of selenium from water. North America Metals Council. Report Compiled by Tom Sandy and Cindy DiSante, CH2MHILL, Charlotte, NC
- Nannipieri P, Muccini L, Ciardi C (1983) Microbial biomass and enzyme activities: production and persistence. *Soil Biol Biochem* 15:679–685. [https://doi.org/10.1016/0038-0717\(83\)90032-9](https://doi.org/10.1016/0038-0717(83)90032-9)
- Ngwenya N, Chirwa EMN (2010) Single and binary component sorption of the fission products Sr²⁺, Cs⁺ and Co²⁺ from aqueous solutions onto sulphate reducing bacteria. *Miner Eng* 23:463–470. <https://doi.org/10.1016/j.mineng.2009.11.006>
- Niu Z, Pan H, Guo X, Lu D, Feng J, Chen Y, Tou F, Liu M, Yang Y (2018) Sulphate-reducing bacteria (SRB) in the Yangtze Estuary sediments: abundance, distribution and implications for the bioavailability of metals. *Sci Total Environ* 634:296–304. <https://doi.org/10.1016/j.scitotenv.2018.03.345>
- Ophardt C (2007) Electron Transport. In: White D (ed) *The physiology and biochemistry of prokaryotes*. Oxford University Press, New York, pp 120–148
- Oulhote Y, Tertre A, Etchevers A, Bot B, Lucas JP, Mandin C, Strat Y, Lanphear B, Glorennec P (2013) Implications of different residential lead standards on children's blood lead levels in France: predictions based on a national cross-sectional survey. *Int J Hyg Environ Health* 216:743–750. <https://doi.org/10.1016/j.ijheh.2013.02.007>
- Papp A, Pecze L, Szabó A, Vezér T (2006) Effects on the central and peripheral nervous activity in rats elicited

- by acute administration of lead, mercury and manganese, and their combinations. *J Appl Toxicol* 26:374–380. <https://doi.org/10.1002/jat.1152>
- Peens J, Wu YW, Brink HG (2018) Microbial Pb(II) precipitation: the influence of elevated Pb(II) concentrations. *Chem Eng Trans* 64:583–588. <https://doi.org/10.3303/CET1864098>
- Rinkes ZL, Deforest JL, Weintraub MN (2014) Interactions between leaf litter quality, particle size, and microbial community during the earliest stage of decay. *Biogeochemistry* 117:153–168. <https://doi.org/10.1007/s10533-013-9872-y>
- Russell MW, Vincent TJ (1998) A review of worldwide approaches to the use of additives to prevent exhaust valve seat recession, in. In: 4th Annual annual Fuels & Lubes Asia conference
- Saiz BL, Barton LL (1992) Transformation of Pb II to lead colloid using *Moraxella bovis*, in. In: American society of microbiology meeting. Abstract No. 347.
- Shamsuddin M (2016) Physical chemistry of metallurgical processes. Wiley, Hoboken. <https://doi.org/10.1002/9781119078326>
- Simon J, Klotz MG (2013) Diversity and evolution of bioenergetic systems involved in microbial nitrogen compound transformations. *Biochim Biophys Acta* 1827:114–135. <https://doi.org/10.1016/j.bbabi.2012.07.005>
- Singh V, Chauhan PK, Kanta R, Dhewa T, Kumar V (2014) Isolation and characterization of pseudomonas resistant to heavy metals contaminants. *Int J Pharm Sci Rev Res* 3:164–167
- Statista (2018) Lead reserves worldwide by country 2017 (in million metric tons). <https://www.statista.com/statistics/273652/global-lead-reserves-by-selected-countries/> . Accessed 5 Aug 2018
- Supanopas P, Sretarugsa P, Krautrachue M, Pokethitiyook P, Upatham ES (2005) Acute and subchronic toxicity of lead to the spotted babylon, *Babylonia Areolata* (Neogastropoda, Buccinidae). *J Shellfish Res* 24:91–98. [https://doi.org/10.2983/0730-8000\(2005\)24%5b91:AASTOL%5d2.0.CO;2](https://doi.org/10.2983/0730-8000(2005)24%5b91:AASTOL%5d2.0.CO;2)
- Taylor MP, Camenzuli D, Kristensen LJ, Forbes M, Zahran S (2013) Environmental lead exposure risks associated with children's outdoor playgrounds. *Environ Pollut* 178:447–454. <https://doi.org/10.1016/j.envpol.2013.03.054>
- Tendenedzai JT, Brink HG (2019) The effect of nitrogen on the reduction of selenite to elemental selenium by *Pseudomonas stutzeri* NT-I. *Chem Eng Trans* 74:529–534. <https://doi.org/10.3303/CET1974089>
- United Nations Environment Programme (2010) Final review of scientific information on lead. United Nations Environment Programme, Nairobi
- Vanýsek P (2011) Electrochemical series. *Handbook of Chemistry and Physics*. CRC Press, London, pp 5-80–5-89
- Verma A, Bishnoi NR, Gupta A (2017) Optimization study for Pb(II) and COD sequestration by consortium of sulphate-reducing bacteria. *Appl Water Sci* 7(5):2309–2320. <https://doi.org/10.1007/s13201-016-0402-7>
- Wade R, DiChristina TJ (2000) Isolation of U(VI) reduction-deficient mutants of *Shewanella putrefaciens*. *FEMS Microbiol Lett* 184:143–148. [https://doi.org/10.1016/S0378-1097\(00\)00011-2](https://doi.org/10.1016/S0378-1097(00)00011-2)
- Wang LK, Hung Y-T, Shammas NK (2004) *Handbook of environmental engineering: physicochemical treatment processes*, vol 3. Humana Press, Totowa. <https://doi.org/10.1385/1-59259-820-x:635>
- Wang H, Cheng H, Wang F, Wei D, Wang X (2010) An improved 3-(4,5-dimethylthiazol-2-yl)-2,5-diphenyl tetrazolium bromide (MTT) reduction assay for evaluating the viability of *Escherichia coli* cells. *J Microbiol Methods* 82:330–333. <https://doi.org/10.1016/j.mimet.2010.06.014>
- Yong P, Rowson NA, Farr JPG, Harris IR, Macaskie LE (2002) Bioreduction and biocrystallization of palladium by *Desulfovibrio desulfuricans* NCIMB 8307. *Biotechnol Bioeng* 80:369–379. <https://doi.org/10.1002/bit.10369>